Theoretical study of quasi-phase-matching fourth harmonic generation in periodically poled lithium tantalate

Wei Xie (谢 威), Xianfeng Chen (陈险峰), Like He (何利科), Yuping Chen (陈玉萍), and Yuxing Xia (夏宇兴)

Institute of Optics & Photonics, Department of Physics; The State Key Laboratory on Fiber Optic Local Area Communication Networks and Advanced Optical Communication Systems, Shanghai Jiaotong University, Shanghai 200240

Received June 16, 2004

The direct fourth harmonic generation (FHG) is theoretically demonstrated based on quasi-phase-matching (QPM) configuration in periodically poled lithium tantalate (PPLT). The wavelength dependence of the period of FHG QPM gratings is calculated. Bandwidths of fundamental wavelength, temperature, and incident angle are also studied. A very wide bandwidth, as large as 119.5 nm, of fundamental wavelength near 3699 nm is found with the QPM period of 9.442 μm and the crystal length of 1 cm.

OCIS codes: 190.0190, 260.1180.

The theory of quasi-phase-matching (QPM)[1] has been widely used in optical frequency conversions[2] and other areas. Compared with the conventional birefringence phase matching (BPM), QMP technology offers lots of novel features, such as relatively high efficiency, no walk-off effect, and large angle tolerance. With the development of the electrical poling technique, we can fabricate the domain-inverted QPM grating with any kinds of periods. In QPM crystal, the polarization direction of the incident light is adjusted to consist with c-axis, in which the largest component of the nonlinear coefficient d_{33} is utilized. In addition, the fact that the QPM crystal will not be affected by the walk-off effect enables us to get higher efficiency with longer QPM crystal. With the periodically poled ferroelectric crystals including lithium niobate and lithium tantalate, the new coherent light can be obtained from the second-order nonlinear process such as optical parameter oscillation (OPO), differential frequency generation (DFG), and second harmonic generation (SHG).

Because of the small fourth-order nonlinear coefficient of the nonlinear crystal, the fourth-order harmonic generation (FHG) has not been paid enough attention during the past years. Another factor that limited the practical application of the FHG is the lack of ferroelectric material with considerable birefringence effect. In direct FHG process, the phase-matching condition of BPM is $n_o^{\omega} = n_e^{4\omega}$. However, in the transparent range of the $LiTaO_3$, the refractive index has the following relation: $n_o^{\omega} < n_e^{4\omega}$. Therefore, the phase-matching condition of the FHG process cannot be achieved with conventional BPM scheme. The alternative way to achieve FHG is the cascaded SHG scheme, which employs the output wave of the first SHG process as the fundamental wave of the second SHG process to obtain the fourth-order harmonic wave. The cascading scheme can be fulfilled in both BPM[3−7] and QPM[8−10] crystals. Figure 1(a) shows the characteristic of the cascading QPM FHG.

As is well known, not only the second-order nonlinear tensor, but also the fourth-order tensor are modulated by the poling field in the periodically poled ferroelectric crystals. Therefore, it is possible to fulfill higher order nonlinear process in QPM crystals.

In this paper, we theoretically analyze the characteristic of the QPM FHG in periodically poled $LiTaO_3$ (PPLT), including the relation between the QPM period and the fundamental wavelength, the angle tolerance, and the temperature tolerance, etc..

As shown in Fig. 1(b), the QPM FHG process is generated in PPLT, where the FHG process can be explained and calculated through the coupled-wave equations. Under the small-signal approximation, the fourth-order harmonic can be expressed as

$$I_{4\omega}(L) = BI_{\omega}^{4}(0)L^{2}\sin c^{2}(\Delta k' L/2), \quad (1)$$

where $B = \frac{2\omega^2(\chi^{(4)})^2}{\pi^2 n_{4\omega} n_{\omega}^4 c^5 \varepsilon_0^3}$ is a constant determined by the material properties, $I_{\omega}(0)$ is the power of fundamental wave, L is the length of the crystal, n_{ω} ($n_{4\omega}$) is the

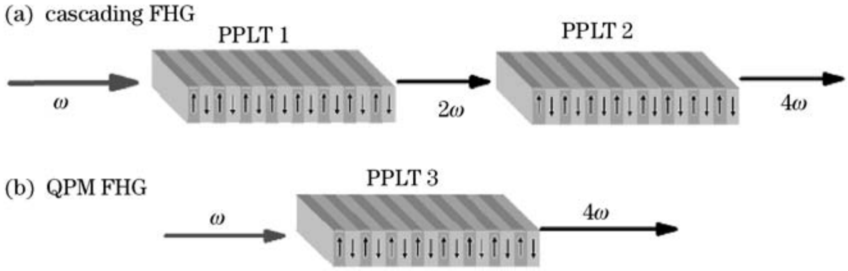

Fig. 1. Schematic diagram of cascading FHG (a) and direct QPM FHG (b) in PPLTs. The sign of fourth (second) nonlinear optical tensor $\chi^{(4)}$ ($\chi^{(2)}$) in PPLT is periodically changed. The periods of three PPLTs are different.

refractive index of the fundamental (fourth-order harmonic) wave, ω is the angle frequency, c is the velocity of light, $\chi^{(4)}$ is the nonlinear tensor. If Λ_1 is the period of the QPM grating, $\Delta k' = k_{4\omega} - 4k_\omega - \frac{2\pi}{\Lambda_1}$ is the wave-vector mismatch. When the condition

$$\Lambda_1 = \frac{\lambda_\omega}{4(n_{4\omega} - n_\omega)} \tag{2}$$

is matched, the wave-vector mismatch $\Delta k' = 0$, where λ_ω is the wavelength of the fundamental wave.

In this paper, we assume the fundamental wave and the fourth-order harmonic incident from the left side of the crystal as an extraordinary light. The refractive index of the light n_e is given by the Sellmeier equation[11]

$$\begin{aligned} n_\mathrm{e}^2 = 4.5299 + &\frac{(0.084752 + 1.7299 \times 10^{-7}F)}{\lambda^2 - (0.2034 - 4.7733 \times 10^{-7}F)} \\ &-8.3146 \times 10^{-8}F - 0.02379\lambda^2, \\ F = (T - 25)&(T + 25 + 546). \end{aligned} \tag{3}$$

Because of the fluctuation of the temperature and variation of the wavelength, the wave-vector mismatch Δk, is not bound to be 0.

From the equations above, we can get the wavelength and temperature tolerance of the QPM FHG in PPLT. Figure 2 shows the relation between the grating period and the fundamental wave in PPLT at temperature of 100 °C. In our calculation, the fundamental wavelength varies from 1.0 to 6.5 μm. In short wavelength band, the QPM period becomes larger as the wavelength increases in order to ensure the phase-matching conditions. The wavelength dependence, however, is changed when the fundamental wavelength increases to 3699 nm, where the corresponding period is 9.442 μm. After that, the QPM period decreases with the increase of the wavelength, which is different to that of the QPM SHG. In SHG process, the QPM period consistently increases as the wavelength increases[12].

Recently, the QPM FHG process (type I) of oo-e scheme has been reported[13], where the nonlinear coefficient d_{31} is employed[4]. Similarly, it can be expected that the bandwidth of the fundamental wavelength will be very large in the inflection point. When the phase-matching condition is strictly satisfied ($\Delta k' = 0$), we get the highest conversion efficiency. However, with the variation of the temperature, incident angle, and fundamental wavelength, the conversion efficiency (or the output fourth-order harmonic power) will be reduced. If the output power decreases to half of the maximum, we define the variation value as the bandwidth (or tolerance) for the temperature, incident angle, or the fundamental wavelength, respectively. The calculated wavelength bandwidth is shown in Fig. 3, where the temperature is fixed at 100 °C and the length of the PPLT crystal is 1 cm. When the fundamental wavelength is about 2467 nm (Λ_1 = 6.818 μm), the bandwidth $\Delta\lambda$ = 0.92 nm. Comparatively, the bandwidth at 3699 nm is $\Delta\lambda$ = 119.5 nm. The insets of Fig. 3 show the wavelength dependence of the normalized output power at 2467 and 3699 nm, respectively. As we can see from the inserts, the output power decreases sharply with the fluctuation of the fundamental wavelength at 2467 nm. In contrast, the normalized output power is stable in a broad band.

Likewise, we discuss the temperature dependence of the FHG in PPLT. The standard work temperature is

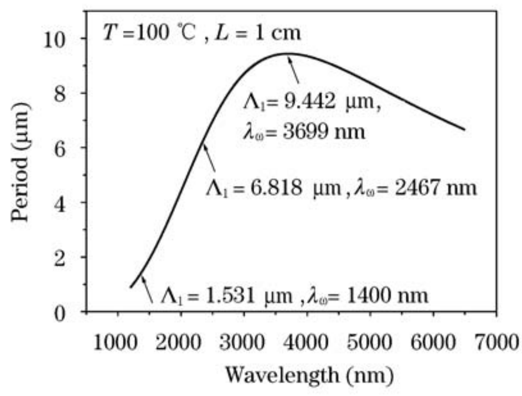

Fig. 2. The period of QPM gratings of PPLT as a function of fundamental wavelength at the temperature of 100 °C. The length of the crystal is 1 cm. The maximum period is $\Lambda = 9.442$ μm at the wavelength of 3699 nm.

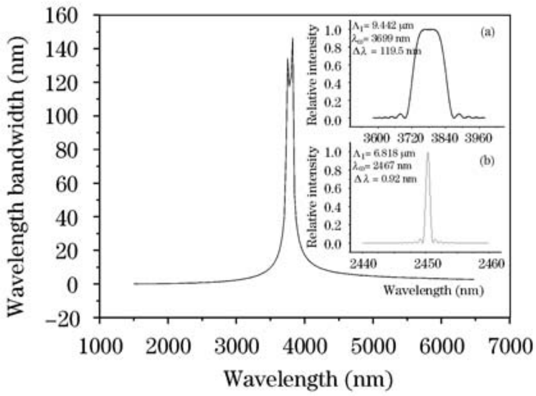

Fig. 3. The bandwidth of QPM FHG versus fundamental wavelength. The temperature is 100 °C and the length of PPLT is set to 1 cm. The insets (a) and (b) are the wavelength dependence of relative intensity of QPM FHG at the central wavelengths of 2467 and 3699 nm, respectively.

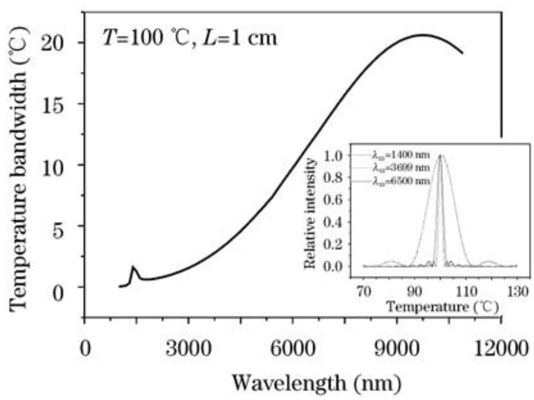

Fig. 4. The calculated temperature bandwidth versus fundamental wavelength at the temperature of 100 °C and the length of 1 cm. The inset shows the effect of temperature variety on the conversion efficiency at the wavelengths of 1400, 3699, and 6500 nm, and the temperature bandwidths are 1.62, 2.69, and 11.69 °C.

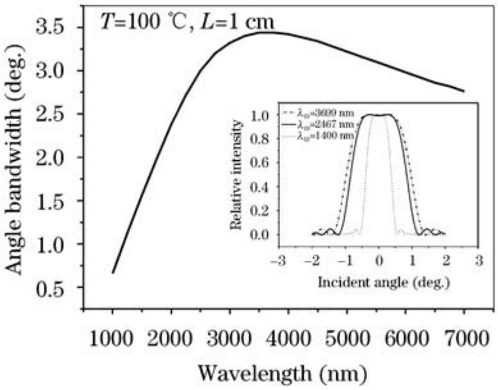

Fig. 5. The calculated results of incident angle bandwidth versus fundamental wavelength. The temperature is 100 °C and the length of PPLN is set to 1cm. The relative intensity as a function of the incident angle of the fundamental wave is displayed in the inset of the figure at the wavelengths of 1400, 2467, and 3797 nm, and the angle bandwidths are 1.38°, 2.96°, and 3.44°, respectively.

is selected as 100 °C, and the calculation result is shown in Fig. 4. Obviously, the bandwidth for temperature gets larger as the fundamental wavelength increases. The inset shows the relation between normalized power and temperature with fundamental wavelength at 1400, 3699, and 6500 nm, respectively. And their bandwidths for temperature are $\Delta T = 1.62$, 2.69, and 11.69 °C.

In the same way, the angle bandwidth can be easily obtained. As demonstrated in Fig. 5, the angle bandwidth will be the largest if fundamental wavelength is 3699 nm, where incident angle is the include angle of incident beam and the incident plane of the crystal. When the wavelengths are 1400, 2467, and 3699 nm, the angle bandwidths are 1.38°, 2.96°, and 3.44°, respectively.

In our calculation, the conversion efficiencies of the direct QPM FHG and cascading FHG are discussed. We assume that the polarization directions of light beams are all consistent with the c-axis of the PPLT crystal so that the largest nonlinear coefficient d_{33} is utilized. Under the assumptions that the power of fundamental wave and the length of the PPLT crystal in both schemes are equal, the QPM conditions are matched, with the small-signal approximation, we can obtain the conversion efficiencies. The result is

$$\frac{I_{4\omega}^{\text{cascading}}}{I_{4\omega}^{\text{direct}}} = \frac{2^{16}\omega^4}{\pi^4 n_{2\omega}^2 c^4} L^4 \frac{(\chi^{(2)})^6}{(\chi^{(4)})^2} \approx 10^2 \frac{(\chi^{(2)})^6}{(\chi^{(4)})^2}, \tag{4}$$

where $\chi^{(n)}$ is the n-order nonlinear tensor, E_0 is the average electric field intensity. In PPLT, $\chi^{(2)} \approx 27 \times 10^{-12}$ (m/V) and $\chi^{(3)} \approx 10^{-22}$ (m^2/V^2). From the equation $\chi^{(n)}/\chi^{(n-1)} = 1/|E_0|$, we get $\chi^{(4)} \approx 3.7\times10^{-32}$ (m^3/V^3). Based on the above results, the ratio of $I_{4\omega}^{\text{cascading}}$ to $I_{4\omega}^{\text{direct}}$ is about 1. It means that the efficiency of direct FHG is approximately same as that of cascading FHG.

Compared with cascading FHG in PPLT crystal, direct FHG has the same conversion efficiency while providing large bandwidth for fundamental wavelength, temperature, and incident angle. Furthermore, the FHG device based on direct FHG schemes is easier to be fabricated because of the single chip design. Therefore, it can be concluded that direct QPM FHG maybe a new promising approach in achieving new coherence light.

In summary, we have theoretically analyzed the direct QPM FHG in PPLT and given the bandwidth for fundamental wavelength, temperature, and incident angle. In our calculation, the bandwidth for fundamental wavelength at 3699 nm is very large (about 119.5 nm). Based on these results, we have also investigated the conversion efficiency of the direct QPM FHG. The result shows that efficiency of direct FHG is approximately same as that of cascading scheme. With the development of the material science and the poling technique, the application of direct FHG in PPLT and other periodically poled materials maybe more attractive.

This work was supported by the National Natural Science Foundation of China (No. 60477016) and the Foundation for Development of Science and Technology of Shanghai (No. 02DJ14001 and 04DZ14001). X. Chen is the author to whom the correspondence should be addressed, his e-mail address is xfchen@sjtu.edu.cn.

References

1. J. A. Armstrong, N. Bloembergen, J. Ducuing, and P. S. Pershan, Phys. Rev. **127,** 1918 (1962).
2. L. E. Myers, R. C. Eckardt, M. M. Fejer, R. L. Byer, W. R. Bosenberg, and J. W. Pierce, J. Opt. Soc. Am. B **12,** 2102 (1995).
3. J. Webjorn, in *Proceedings of 8th European Conference on Integrated Optics* 492 (1997).
4. Y. Suzuki, S. Ono, H. Murakami, T. Kozeki, H. Ohtake, N. Sarukura, G. Masada, H. Shiraishi, and I. Sekine, Jpn. J. Appl. Phys. Lett. **41,** 823 (2002).
5. J. L. He, X. Q. Lu, Y. L. Jia, B. Y. Man, S. N. Zhu, and Y. Y. Zhu, Acta Phys. Sin. **49,** 2106 (2000).
6. J. H. Lu, G. L. Wang, Z. Y. Xu, C. T. Chen, J. Y. Wang, C. Q. Zhang, and Y. G. Liu, Chin. Phys. Lett. **19,** 680 (2002).
7. T. Kojima, S. Konno, S. Fujikawa, and K. Yasui, Electrical Engineering in Japan **137,** 18 (2001).
8. L. B. Shama, H. Daido, Y. Kato, S. Nakai, T. Zhang, Y. Mori, and T. Sasaki, Appl. Phys. Lett. **69,** 3812 (1996).
9. Y. Deyanova, S. Saltiel, and K. Koynov, Opt. Commun. **178,** 437 (2000).
10. O. Pfister, J. S. Wells, L. Hollberg, L. Zink, D. A. Van-Baak, M. D. Levenson, and W. R. Bosenberg, Opt. Lett. **22,** 1211 (1997).
11. J. P. Feve and B. Boukanger, Phys. Rev. A **65,** 063814 (2002).
12. K. S. Abedin, J. Appl. Phys. **80,** 6561 (1996).
13. Y. P. Chen, X. F. Chen, S. W. Xie, X. L. Zeng, Y. X. Xia, and Y. L. Chen, J. Opt. A: Pure and Appl. Opt. **4,** 324 (2002).
14. N. E. Yu, J. H. Ro, M. Cha, S. Kurimura, and T. Taira, Opt. Lett. **27,** 1046 (2002).